Journal of Thermal Analysis and Calorimetry (2022) 147:6901–6912
https://doi.org/10.1007/s10973-021-10976-z

Numerical investigation of the stagnation point flow of radiative magnetomicropolar liquid past a heated porous stretching sheet

A. S. Warke[1] · K. Ramesh[1] · F. Mebarek-Oudina[2] · A. Abidi[3,4,5]

Received: 11 March 2021 / Accepted: 29 June 2021 / Published online: 25 July 2021

Abstract

In this paper, we have investigated the two-dimensional magnetohydrodynamic steady boundary layer flow of a viscous magnetomicropolar liquid via an extending area. The impact of heat sink/source and chemical reaction is considered. The governing equations are modeled in Cartesian coordinate system. Using the suitable similarity transformations, the partial differential equations system is changed into the nonlinear ordinary differential equations system. The resulting system of equations is solved via mathematical renowned software Mathematica. The impact of diverse parameters through microrotation, concentration, temperature and velocity is examined via graphs. The present study reveals that the velocity is rising function of Soret number, Richardson number and Grashof number. It is mentioned that the greater velocity is located in the case of Newtonian liquid in contrast with the micropolar liquid. In the absence of chemical reaction parameter, the velocity is more as compared with higher chemical reaction parameter. Radiation, Hartmann and chemical reaction parameters augment the temperature. Concentration is a reducing function of radiation, Hartmann and chemical reaction parameters.

Keywords Magnetomicropolar liquid · Stretching sheet · Partial differential equations · Radiation · Heat source/sink

Abbreviations

B_0	Magnetic field strength [Tesla]
C	Concentration of the liquid [mol m^{-3}]
C_p	Specific heat at constant pressure [J kg^{-1} K^{-1}]
c_s	Concentration susceptibility
D	Mass diffusivity coefficient [m^2 s^{-1}]
Du	Dufour number [–]
j	Microinertia density [J m^{-3}]
g	Acceleration due to gravity [m s^{-2}]
K_T	Thermal diffusive ratio [–]
k^*	Mean absorption coefficient [m^{-1}]
K_c^*	Reaction rate [mol m^{-3} s^{-1}]
K_p^*	Permeability parameter [m^2]
M	Hartmann number [–]
N	Microrotation vector
Pr	Prandtl number [–]
q_r	Dimensional radiative heat flux [W m^{-2}]
R	Radiation parameter [–]
Sc	Schmidt number [–]
Sr	Soret number [–]
T	Fluid temperature [K]
T_∞	Free-stream temperature [K]
u, v	Velocity components [m s^{-1}]
α	Thermal diffusivity [m^2 s^{-1}]
υ	Kinematic [m^2 s^{-1}]
β_c	Concentration expansion coefficient [K^{-1}]
β_T	Thermal expansion coefficient [K^{-1}]
γ	Chemical reaction parameter [–]
σ	Electrical conductivity [S m^{-1}]
μ	Dynamic viscosity [kg m^{-1} s^{-1}]
ρ	Fluid density [kg m^{-3}]
κ	Vortex viscosity
ψ	Stream function [–]
σ_1	Stefan–Boltzmann constant [W m^{-2} K^{-4}]
Γ	Micropolar fluid parameter

✉ F. Mebarek-Oudina
oudina2003@yahoo.fr; f.mebarek_oudina@univ-skikda.dz

[1] Mathematics Department, Symbiosis Institute of Technology, Symbiosis International (Deemed University), Pune 412115, India

[2] Department of Physics, Faculty of Sciences, University of 20 Août 1955-Skikda, Skikda 21000, Algeria

[3] Physics Department, College of Sciences Abha, King Khalid University, Abha, Saudi Arabia

[4] Research Laboratory of Metrology and Energy Systems, National Engineering School, Energy Engineering Department, Monastir University, Monastir, Tunisia

[5] Higher School of Sciences and Technology of Hammam Sousse, Sousse University, Sousse, Tunisia

θ Temperature [–]
λ Richardson number [–]
δ Concentration Grashof number [–]

Introduction

The effect of radiation has vast applications in engineering processes and science. The radiation due to heat transport on various fluid motions is crucial in high temperature processes and space technology. Thermal radiation effect can also play an salient position in administering heat transport in polymer manufacturing industry, where the satisfactory of the ultimate product depends, to some extent to the heat controlling aspects. Power generation systems, liquid metal fluids, nuclear reactors and high temperature plasmas are some more significant applications of radiative heat transport. For these, many researchers have made their contributions to find out about of radiation liquid flow. Sui et al. [1] have inspected the mass and heat transport of viscoelasticity-based micropolar liquid past an extending surface under the slip conditions effect. Mahabaleshwar et al. [2] have scrutinized the impact of heat transport on the Walters' liquid B motion past extending surface under the impact of Navier slip boundary condition with porous medium. Chiu et al. [3] have reported the convective energy transport in parallel rectangular ducts under the radiation effect. Hayat et al. [4] have examined the influence of Brownian and thermophoresis motion through the melting transport of magnetized nanoliquid past extending sheet with heat sink /source. Sheikholeslami et al. [5] have explored the impact of nanoparticles (*NPs*) through heat transport performance of phase change material (PCM) in solidification development with radiation. Waqas et al. [6] have reported the impact of convective boundary condition, Joule heating and viscous dissipation over the motion of micropolar liquid past extended sheet. Zheng et al. [7] have scrutinized the boundary layer flow and radiative transport of an incompressible micropolar liquid through an extending/shrinking surface. Hsiao [8] scrutinized the influences of viscous dissipation through the magnetized micropolar nanofluid movement over an extending surface. Mabood et al. [9] have reported the mass and heat transport motion of a micropolar liquid through an extending area surrounded in a non-Darcian permeable media with Soret effect and radiation. Bhattacharya et al. [10] have scrutinized the micropolar liquid motion through a permeable shrinking plate under the influence of radiation. Reddy and Sandeep [11] have studied the impact of injection /suction and radiation on Carreau liquid movement past a porous stretching plate with convective slip conditions effect. Shateyi et al. [12] have studied the impact of radiation and Hall currents through magnetohydrodynamic combined convective motion on a perpendicular sheet in porous media. Pal and Mondal [13] have scrutinized the influence of chemical reaction and radiation resting on the magnetohydrodynamic non-Darcy unsteady combined convection transfer of energy and mass past extending plate. Sohail et al. [14] have utilized an optimal homotopy analysis procedure to investigate the Maxwell nanoliquid flow with various effects such as gyrotactic microorganism, entropy generation and radiation. In recent days, Generalized Differential Quadrature Method (GDQM) is extensively used in the fluid flow systems since it is a strong method. Many researchers have tested their numerical examples with GDQM and received superb convenience, accuracy and efficiency. Hayat et al. [15] have constructed a model for the unsteady radiative propulsion of Maxwell nanomaterial over the stretched sheet. In view of this, Qasim et al. [16] have used generalized differential quadrature method to discuss the boundary layer motion of Jeffrey liquid on a stretching disk through thermal radiation. To check the reliability and validity of the current model, the comparison study is made with the help of Chebyshev–Gauss–Lobatto spectral technique. Dogonchi et al. [17] have discussed the motion of nanofluid within the partially heated rhombus cavity with thermal radiation using control volume finite difference technique. Few more studies can be seen in [18–25] in the direction of liquid flow situation with thermal radiation effect.

Understanding of the procedure of magnetic field generation through self-inductive motion in electrically conducting fluids has superior dramatically over the closing few decades. Magnetic effect on the fluid flows has been a vast topic of interest in physics. Principally, the MHD flows allied with heat transport have received much curiosity, because of their applications in various industrial areas, such as microelectronic devices, crystal growth in fluids, electronic packages and electric propulsion for space discovery. In view of these things in mind, it is essential to discuss the important features of transport phenomena in such a procedure so that a better product can be created with improved design. The impact of viscous dissipation and radiation on the magnetohydrodynamic through an oscillating perpendicular sheet bounded in a permeable media under variable surface conditions has been reported through Kishore et al. [26]. Karthikeyan et al. [27] have scrutinized the impact of radiation on magnetohydrodynamic convective motion past an upright sheet in a permeable medium; it was noticed that the enhancement in the radiation parameter involves, reduces in the boundary layer thickness and rises the rate of heat transport. Hossain and Samand [28] have investigated the MHD natural convective activity over an extending surface with radiation and chemical reaction. It was noticed that the concentration description rise like the radiation parameter is enhanced. Hsiao [29] presented a study for the combination impacts of thermal radiation and convection in nanofluid with multimedia physical features. Waqas [30] discussed the ferromagnetic stretching motion of Williamson fluid under the magnetic dipole effects with the help of bvp4c scheme and concluded that the velocity and thermal distributions have in reverse trend for the ferrohydrodynamic interaction parameter. Wakif and Sehaqui [31] have discussed the nanofluid flow situation horizontal planar configuration by considering MHD effects using generalized differential quadrature method. In today's society, mathematical software programs are widely using for complex problems. Mathematica is a significant computer algebra system to use, especially solving the complex differential equations (DEs). NDSolve in mathematics designates the solutions for the functions as interpolating function objects. NDSolve currently utilizes the numerical technique of lines to compute solutions to DEs. Many in-built commands are available in NDSolve such as shooting and Runge–Kutta techniques. In view of this, many authors have used the computational software Mathematica/MATLAB for many fluid flow situations. For instance, Naz et al. [32] have provided the numerical solutions for the motion of MHD Carreau nanoliquid over the cylinder with the help of computational software Mathematica. Khan et al. [33] have provided MATLAB results through Built-in-Shooting method for the motion of nanoliquid through rotating disks under the magnetohydrodynamic effects. Some more related important studies can be found in the articles [34–63]. Magnetic field along with radiation plays a significant role in science and engineering branches, for instance, the regulation of the diurnal rhythms, circadian system, melatonin secretion, telecommunications, electrical equipment and electrical power transmission systems. Keeping many applications, the researchers have started their work in radiative and magnetic fields in the fluid flow systems. Kumar et al. [64] have utilized shooting and Runge–Kutta methods to study the MHD radiative flow of Casson liquid through an exponentially stretching area. Golafshanand Rahimi [65] have provided homotopy analysis solutions for the motion of MHD third-grade nanoliquid through a stretching sheet and radiation effects. Wakif [66] studied the motion of MHD radiative Casson liquids over elongating elastic sheet using innovative GDQLLM algorithm. Thumma et al. [67] have used GDQM to discuss the flow behavior of Casson liquid through a stretching surface with the influences of MHD and thermal radiation. Few more important studies can be capture through the references [68–74] and the references therein.

The novelty of this work is to bring out the impacts of porous medium through the mass and heat transport of mixed convective radiative magnetomicropolar liquid flow (the motion of micropolar liquid with radiation and magnetic field) past a vertical surface. We consider the flow configuration in Cartesian coordinate system. Using appropriate similarity transformations and dimensional quantities, the complex differential equations may be transformed to a simplified nonlinear system of ODEs. We used the symbolic software Mathematica to resolve the equations system. The graphical results are obtainable for sundry parameters on the temperature, microrotation, velocity and concentration.

Modeling

A steady, 2D, incompressible viscous electrically conducting micropolar liquid near to a stagnation point through a perpendicular hot sheet is considered. The condition of the no-slip boundary is assumed for the liquid medium. The heated plate is maintained at concentration $C_w(x)\left(> C_\infty\right)$ and temperature $T_w(x)\left(> T_\infty\right)$. The movement field is conditional on the same uniform magnetic field B_0 as that concerned standard to the sheet. The magnetic *Re* of the conducting liquid is assumed to be smaller in order that Hall impact and induced magnetic field may be discarded. The physical geometry of the current study is presented in Fig. 1. The aforementioned and usual boundary layer assumptions, the governing momentum, energy and concentration equations for the steady micropolar liquid flow toward a stagnation point are given by [75, 76].

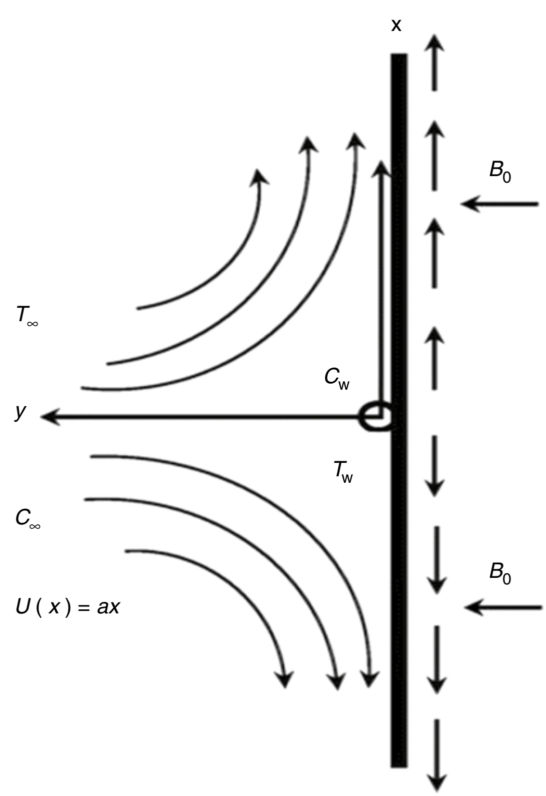

Fig. 1 Physical problem sketch

$$\frac{\partial u}{\partial x} + \frac{\partial v}{\partial y} = 0, \tag{1}$$

$$\rho\left(u\frac{\partial u}{\partial x} + v\frac{\partial u}{\partial y}\right) = \rho U\frac{dU}{dx} + (\mu + k)\frac{\partial^2 u}{\partial y^2} + k\frac{\partial N}{\partial y} + \left(\frac{\sigma B_0^2}{1 + m^2} + \frac{\rho\mu}{K_p^*}\right)(U - u) + \rho g\beta_{\mathrm{T}}\left(T - T_\infty\right) + \rho g\beta_{\mathrm{c}}\left(C - C_\infty\right), \tag{2}$$

$$\rho j\left(u\frac{\partial N}{\partial x} + v\frac{\partial N}{\partial y}\right) = \left(\mu + \frac{k}{2}\right)j\frac{\partial^2 N}{\partial y^2} - k\left(2N + \frac{\partial u}{\partial y}\right), \tag{3}$$

$$\rho C_{\mathrm{p}}\left(u\frac{\partial T}{\partial x} + v\frac{\partial T}{\partial y}\right) = \alpha\frac{\partial^2 T}{\partial y^2} + \frac{DK_{\mathrm{T}}}{c_{\mathrm{s}}}\frac{\partial^2 C}{\partial y^2} - \frac{\partial q_{\mathrm{r}}}{\partial y}, \tag{4}$$

$$u\frac{\partial C}{\partial x} + v\frac{\partial C}{\partial y} = D\frac{\partial^2 C}{\partial y^2} + \frac{DK_{\mathrm{T}}}{T_m}\frac{\partial^2 T}{\partial y^2} - K_{\mathrm{c}}^*\left(C - C_\infty\right). \tag{5}$$

The appropriate boundary conditions may be put as [77]:

$$\left.\begin{array}{l} u = 0,\ \ v = 0,\ \ N = -n\frac{\partial u}{\partial y},\ \ T = T_{\mathrm{w}}(x),\ \ C = C_{\mathrm{w}}(x)\ \text{ at }\ y = 0, \\ u \to U(x),\qquad N \to 0,\qquad T \to T_\infty,\qquad C \to C_\infty\ \text{ as }\ y \to \infty. \end{array}\right\}. \tag{6}$$

We introduce the equations of Cauchy–Riemann as:

$$u = \frac{\partial\psi}{\partial y}, v = -\frac{\partial\psi}{\partial x}. \tag{7}$$

Noted that g is the gravity acceleration, T is the fluid temperature, u, v are velocity for x and y direction, C represents the concentration of the liquid in the boundary layer, υ, μ and k are the kinematic, dynamic and vortex viscosities, respectively, β_{c} is the concentration expansion coefficient, β_{T} is the thermal expansion coefficient, B_0 is the magnetic fields strength, ρ is the fluid density, D is the mass diffusivity coefficient, j is the microinertia density, K_T is the thermal diffusive ratio, α is the thermal diffusivity, K_{c}^* is the reaction rate, K_{p}^* is the permeability parameter, C_{p} denotes the specific heat at constant pressure, N is the microrotation vector, ψ is the stream function, σ is the electrical conductivity, m is Hall current parameter, c_s is the concentration susceptibility and n is a constant such that $0 \le \mathrm{n} \le 1$. The case $n = 0$, is called strong concentration, which indicates $N = 0$ near the wall, represents concentrated particle flows in which the microelements close to the wall surface are unable to rotate. The case $n = 1/2$ indicates the vanishing of anti-symmetric part of the stress tensor and denotes weak concentrations. The case $n = 1$ is used for the modeling of turbulent boundary layer flows. Equation (7) automatically satisfies continuity Eq. (1).

We define the similarity transformations and non-dimensional variables as

$$\eta = \left(\frac{a}{\upsilon}\right)^{1/2}y,\quad f(\eta) = \frac{\psi}{(a\upsilon)^{1/2}x},\quad \omega(\eta) = \frac{N}{a\left(\frac{a}{\upsilon}\right)^{1/2}x},$$

$$\theta(\eta) = \frac{T - T_\infty}{T_{\mathrm{w}} - T_\infty},\quad \varphi(\eta) = \frac{C - C_\infty}{C_{\mathrm{w}} - C_\infty},$$

$$M = \frac{\sigma B_0^2}{\rho a},\quad \lambda = \frac{\mathrm{Gr}}{\mathrm{Re}_{\mathrm{x}}^2},\quad \mathrm{Gr} = \frac{g\beta_{\mathrm{T}}\left(T_{\mathrm{w}} - T_\infty\right)x^3}{\upsilon^2},$$

$$\mathrm{Gc} = \frac{g\beta_{\mathrm{c}}\left(C_{\mathrm{w}} - C_\infty\right)x^3}{\upsilon^2},$$

$$\delta = \frac{\mathrm{Gc}}{\mathrm{Re}_{\mathrm{x}}^2},\quad \mathrm{Re}_{\mathrm{x}} = \frac{\mathrm{ax}}{\upsilon},\quad S_{\mathrm{c}} = \frac{\upsilon}{D},\quad R = \frac{4\sigma_1 T_\infty^3}{\alpha k^*},$$

$$K_{\mathrm{p}} = \frac{\upsilon}{aK_{\mathrm{p}}^*},\quad \mathrm{Pr} = \frac{\mu C_{\mathrm{p}}}{\alpha},$$

$$\mathrm{Du} = \frac{\mathrm{DK_T}\left(C_{\mathrm{w}} - C_\infty\right)}{C_{\mathrm{s}}C_{\mathrm{p}}\mu\left(T_{\mathrm{w}} - T_\infty\right)},\quad \mathrm{Sr} = \frac{\mathrm{DK_T}\left(T_{\mathrm{w}} - T_\infty\right)}{T_{\mathrm{m}}\nu\left(C_{\mathrm{w}} - C_\infty\right)},\quad \Gamma = \frac{k}{\mu}. \tag{8}$$

Moreover, the radiative heat flux q_{r} is explained through Rosseland approximation like:

$$q_{\mathrm{r}} = -\frac{dT^4}{dy}\frac{4\sigma_1}{3k^*}, \tag{9}$$

in which σ_1 and k^* are the Stefan–Boltzmann constant and the mean absorption coefficient, respectively. The liquid-phase temperature differences inside the flow are supposed to be smaller; hence, T^4 can be stated as a temperature linear function. This is completed through developing T^4 in a Taylor series on the ignoring higher-order terms to yield and free-stream temperature T_∞

$$T^4 = 4T_\infty^3 T - 3T_\infty^4 \tag{10}$$

Using the dimensionless parameters, the similarity transformations and afore mentioned assumptions, Eqs. (2–5) can be converted to the following coupled highly nonlinear ODEs

$$(1+\Gamma)f''' + 1 - f'^2 + ff'' + \Gamma\omega' + \left(\frac{M}{1+m^2} + K_p\right)(-f'+1) + \theta\lambda + \delta\varphi = 0, \tag{11}$$

$$\left(1+\frac{\Gamma}{2}\right)\omega'' + f\omega' - f'\omega - \Gamma(2\omega + f'') = 0, \tag{12}$$

$$\frac{1}{Pr}\left(1+\frac{4}{3}R\right)\theta'' + f\theta' - f'\theta + Du\varphi'' = 0, \tag{13}$$

$$\frac{1}{\mathrm{Sc}}\varphi'' + f\varphi' - f'\varphi - \gamma\varphi + \mathrm{Sr}\theta'' = 0. \tag{14}$$

The dimensionless boundary conditions are

$$\left.\begin{array}{l} f(0)=0,\ f'(0)=0,\ \ \omega(0)=-nf''(0),\ \ \theta(0)=1,\ \ \varphi(0)=1 \text{ at } \eta=0, \\ f'(\eta)\to 1,\qquad \omega(\eta)\to 0,\qquad \theta(\eta)\to 0,\qquad \varphi(\eta)\to 0 \text{ as } \eta\to\infty. \end{array}\right\}. \tag{15}$$

in which, the prime represents the differentiation through respect to η.

Sherwood number Sh, Nusselt number Nu and skin friction coefficient C_f are the physical quantities of the engineering interest, and these are

$$C_f = \frac{\tau_w}{\rho U^2/2},\quad Nu = \frac{xq_w}{(T_w - T_\infty)\alpha},\quad Sh = \frac{xM_n}{D(C_w - C_\infty)}. \tag{16}$$

The heat flux q_w, wall shear stress τ_w and mass flux M_n are represented by

$$\tau_w = \left((\mu+k)\frac{\partial u}{\partial y} + \mathrm{kN}\right)_{y=0},\quad q_w = -\alpha\left(\frac{\partial T}{\partial y}\right)_{y=0},\quad M_n = -D\left(\frac{\partial C}{\partial y}\right)_{y=0}, \tag{17}$$

and with the help of similarity transformations, we get

$$\frac{1}{2}C_f\mathrm{Re}_x^{1/2} = \left(1+\frac{\Gamma}{2}\right)f''(0) + \Gamma\omega(0),\quad \frac{Nu}{\mathrm{Re}_x^{1/2}} = -\theta'(0),\quad \frac{Sh}{\mathrm{Re}_x^{1/2}} = -\phi'(0). \tag{18}$$

Results with discussion

Equations (11–14) in the company of the boundary conditions (15) are extremely nonlinear. It is complicated to resolve the system of equations analytically. For this reason, we have opted Mathematica software by shooting technique to solve the equations system. This part is intended to see the behavior of various liquid parameters as Schmidt number Sc, Hartmann number M, Prandtl number Pr, Dufour number Du, R, Sr, γ, micropolar fluid parameter Γ, temperature Richardson number λ and concentration Grashof number δ on the diverse flow quantities such as velocity, temperature, concentration and microrotation distributions. Moreover, in the current study the mentioned liquid physical parameters have been chosen as follow: $1 \le R \le 4,\ 3 \le \mathrm{Sr} \le 6,\ 1 \le \lambda \le 4,\ 0 \le \Gamma \le 9,\ 0 \le \gamma \le 3,$ $1 \le \delta \le 4,\ 4 \le \mathrm{Pr} \le 7,\ 1 \le M \le 4,\ 0.4 \le \mathrm{Du} \le 0.7$ and $2 \le \mathrm{Sc} \le 5$. It is observed from our analysis that the Newtonian liquid model outcomes can be captured through locale $\Gamma = 0$ in the current study.

Figure 2 is designed to see the variations in velocity profiles for diverse fluid flow parameters for instance, Prandtl number Pr, radiation parameter R, micropolar fluid parameter Γ, concentration Grashof number δ, chemical reaction parameter γ and temperature Richardson number λ. From Fig. 2(a), the velocity reduces with rise of radiation parameter R. Obviously, this situation is true because when radiation increases, there is a decrement in the boundary layer thickness, which ultimately reduces the velocity. Figure 2(b) is organized to observe the actions of Soret number via the velocity profile. It is depicted from this figure that velocity is a rising function of Sr. It is because Sr is the temperature difference to the concentration ratio, which means augment in temperature or diminish in concentration leads to augment in Soret number values. Using this phenomenon, it is well known that when the temperature increases, fluid viscosity decreases, which results there is an augment in the velocity curve. The impact of λ via the velocity is provided in Fig. 2(c). Here, the boundary layer velocity enhances with an augment of Richardson. It is physically justified because it is the ratio of Gr to the square of the *Re*https://en.wikipedia.org/wiki/Reynolds_number, *Grashof number* (*Gr*) consists of temperature differences, so that the density decreases due to an increase in temperature differences and causes the fluid to rise. From Fig. 2(d), the velocity reduces with rising values of micropolar fluid parameter. Also, the higher velocities

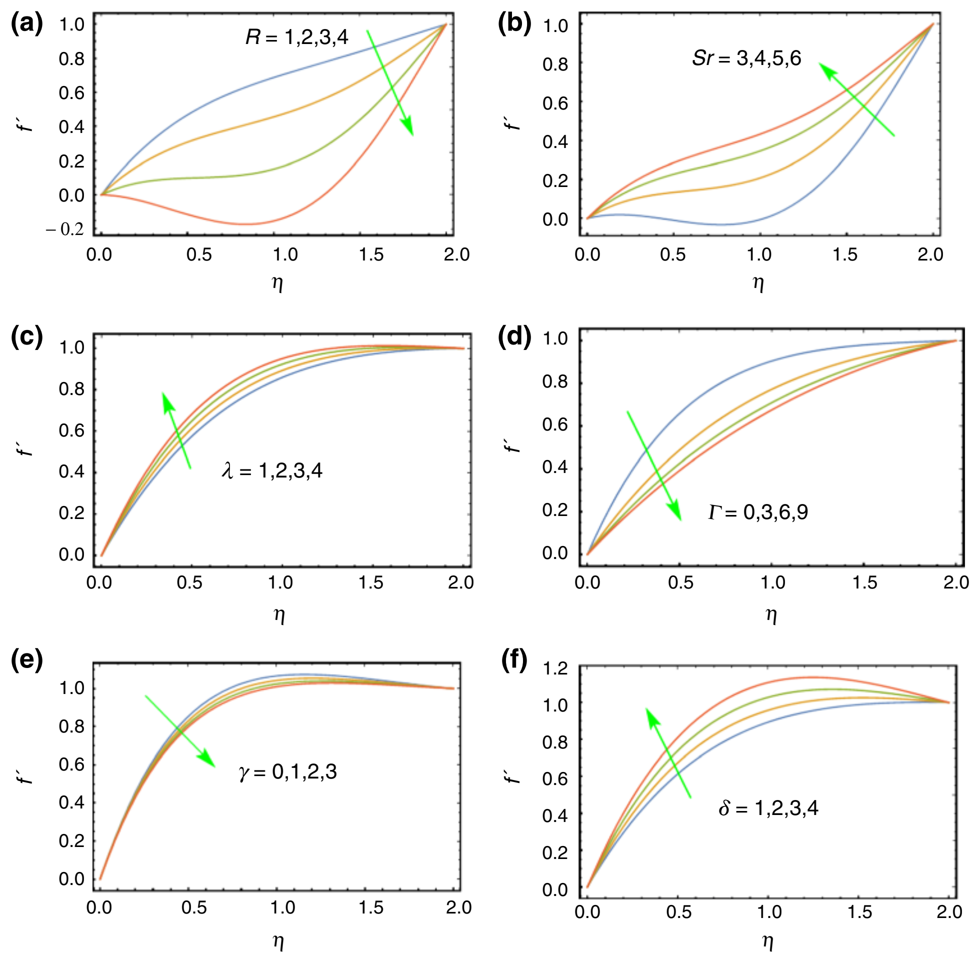

Fig. 2 Diverse fluid flow parameters variations via the velocity profiles

are observed in Newtonian fluid model as distinguished to the micropolar fluid model. Figure 2(e) shows that the velocity reduces with augment of chemical reaction parameter. Furthermore, the greater velocities are determined without chemical reaction parameter. Figure 2(f) demonstrates that, with augment of concentration Grashof number, the velocity increases. The similar trend is determined in many references.

Figure 3 is organized to see the performance of Prandtl number Pr, micropolar fluid parameter Γ, Hartmann number M, R, λ, and Du on the microrotation distribution. It is showed that the microrotation continuously reduces in magnitude through η and becomes zero outlying from the plate. As estimated, the microrotation influences are more dominant near the wall. The similar trend is followed in all the plots means up to certain length the behavior for microrotation; after the critical point, the opposite behavior is observed. The increase in radiation enhances the microrotation up to certain range of transverse direction; thereafter, it follows reverse trend (Fig. 3(a)). From Fig. 3(b) that, the microrotation is reduced up to some critical point; after that, it increases. Increasing values of magnetic strength, the microrotation decreases to the critical point after the situation is different (see Fig. 3(c)). The fact once this, the existence of a magnetic field in an electrically conducting liquid influenced through Lorentz force, which contracts the flow. Figure 3(d) shows that there is a decrement in the microrotation with rise of Richardson number; later, the reverse trend is followed. Micropolar fluid parameter increases the microrotation for the fixed length of transverse direction; later, the situation is reversed (see Fig. 3(e)). The opposite behavior is determined with respect to Dufour number (see Fig. 3(f)).

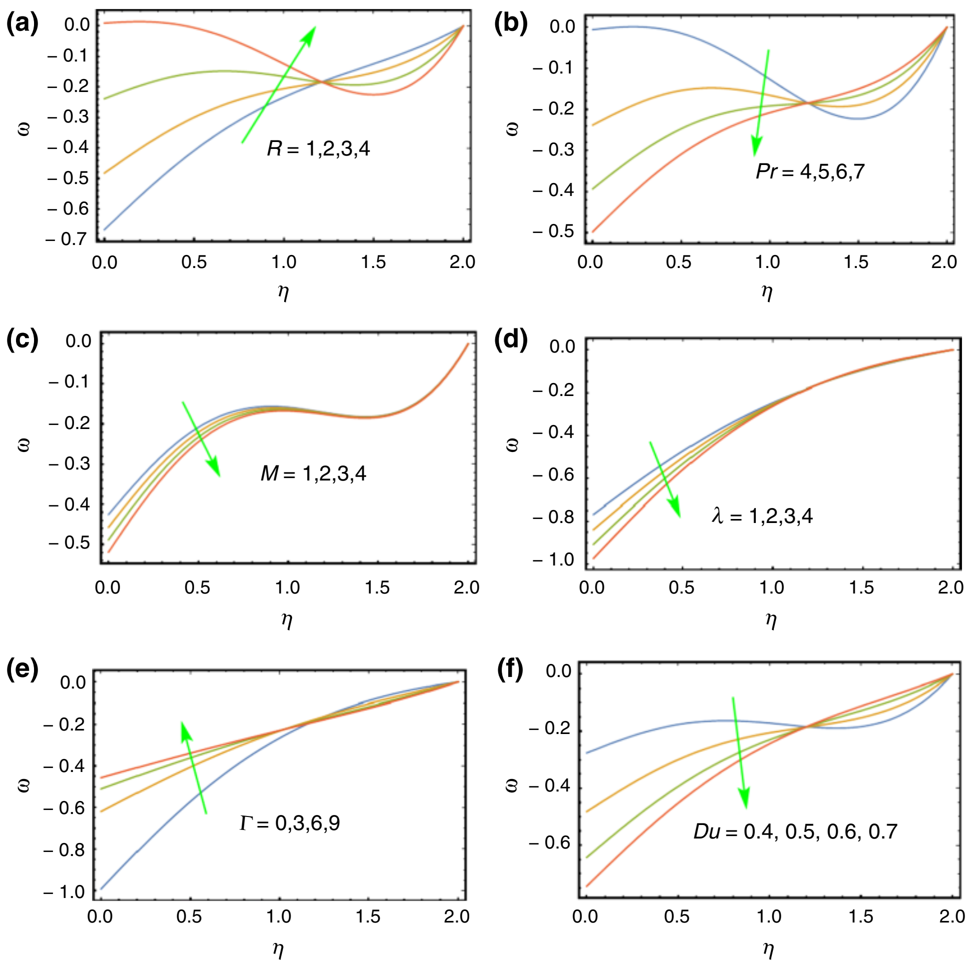

Fig. 3 Diverse fluid flow parameters variations via the microrotation profiles

The behavior of diverse parameters such as radiation parameter R, Soret number Sr, Hartmann number M, Prandtl number Pr, γ and Du via the temperature profiles is exposed in Fig. 4. In all the cases, the temperature is parabolic in nature. Figure 4(a) depicts that the radiation parameter rises the temperature. However, in Fig. 4(b), the higher temperature is seen for lower values of Pr and the trend is reversed for higher Pr. From Fig. 4(c) and (d), the temperature rises with augment of M and γ. The contrary behavior is determined with augment of Dufour number and Soret number to that of Hartmann number (see Fig. 4(e) and (f)). Figure 5 displays the concentration profiles for various fluid flow parameter. Figure 5(a) and (b) shows that the concentration augments with rise of Dufour number and Schmidt number. Radiation parameter reduces the concentration (see Fig. 5(c)). From Fig. 5(d), the concentration enhances with increasing of Prandtl number values. Figure 5(f) and (e) shows the concentration profiles via γ and M, respectively. It is depicted from these figures that the concentration reduces through augment of γ and M.

To check the variations in C_f, local Nu and local Sh through various physical parameters of interest, Tables 1–3

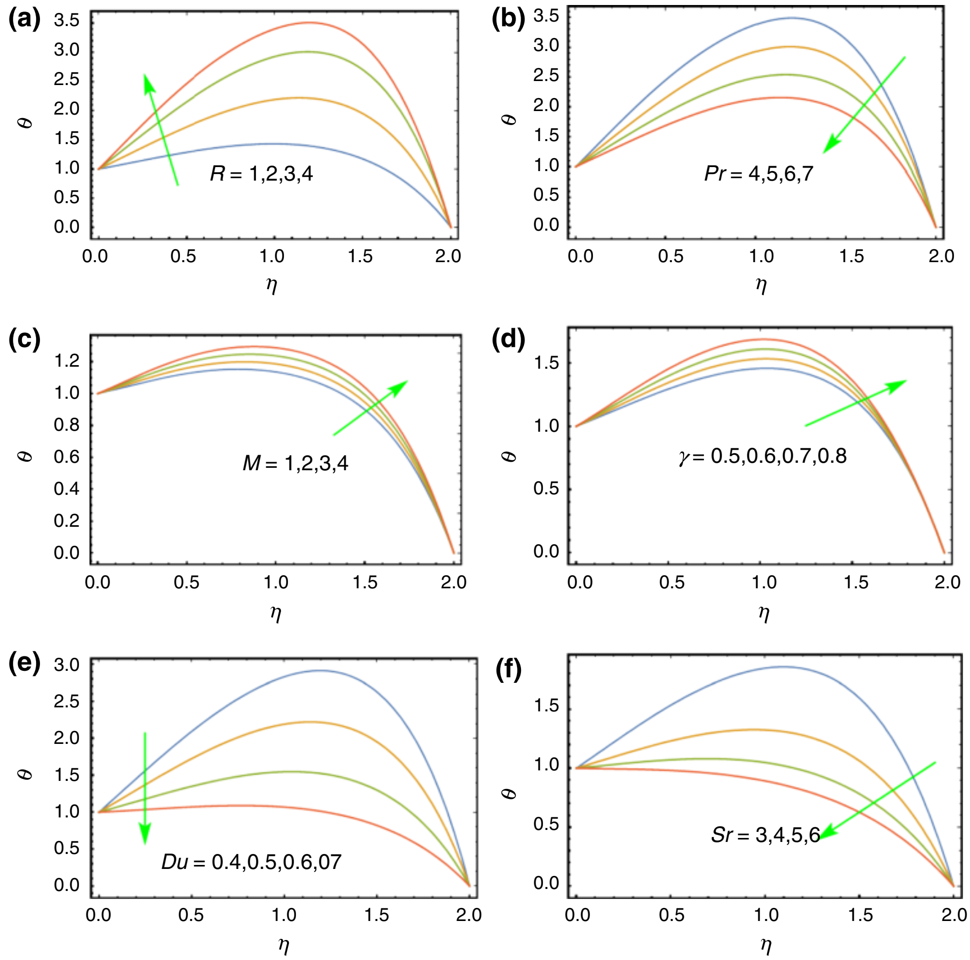

Fig. 4 Diverse fluid flow parameters variations via the temperature profiles

are prepared. Along with these variations, the comparison study is also made via the existing literature Baag et al. [77]. It is noticed that the presented findings are in good agreement through the previous published works as particular cases for specific values of the parameters. Table 1 represents the variations in skin friction coefficient. It is noticed that skin friction reduces with rising values of *Pr* in the absence of buoyancy impact and chemical reaction. Buoyancy forces enhances the skin friction coefficient. Skin friction reduces through rising values of *Sc* and γ. Table 2 is prepared to see the variations in local *Nu*. It is observed that C_f is an rising function of Prandtl number and buoyancy effect. Table 3 shows that local *Sh* rises through increase in γ and buoyancy forces. Thus, it is concluded that lighter diffusive species favoring constructive reaction are appropriate for diminishing mass transport rate at the bounding area.

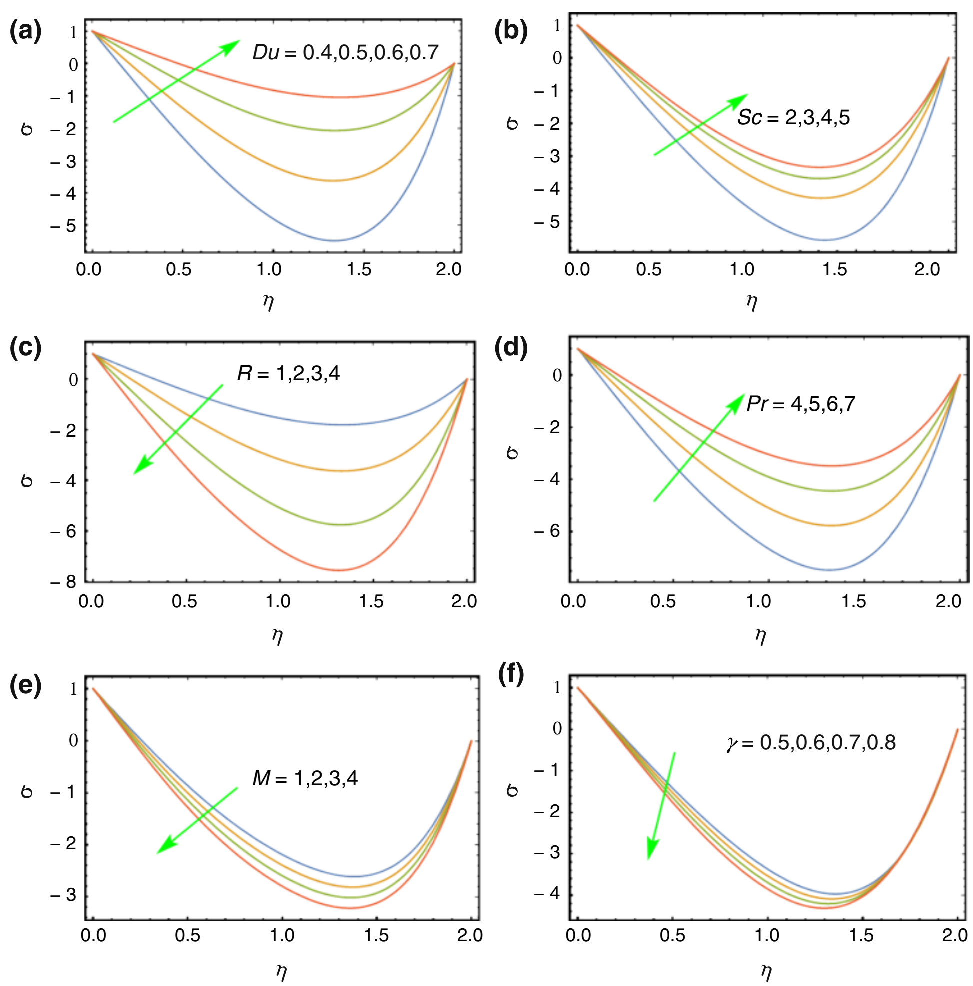

Fig. 5 Diverse fluid flow parameters variations via the concentration profiles

Table 1 Comparison of values of $\frac{1}{2}C_f\mathrm{Re}_x^{1/2}$ for different values of Pr, δ, Sc, γ when $\Gamma = M = K_p = R = Du = Sr = 0$ and $\lambda = 1$.

Pr	δ	Sc	γ	Present results	Baag et al. [77]
0.71	0	0	0	1.68878	1.70328
1	0	0	0	1.66818	1.67490
7	0	0	0	1.52449	1.51800
0.71	1	0	0	2.18466	2.27761
0.71	1	0.22	0	2.15522	2.24014
0.71	1	0.22	1	2.13709	2.21215
1	1	0.22	1	2.11616	2.18747

Table 2 Comparison of values of $\frac{Nu}{\mathrm{Re}_x^{1/2}}$ for different δ *and* Pr when $\Gamma = M = K_p = R = Du = Sr = Sc = 0$ and $\lambda = 1$.

Pr	δ	Present results	Baag et al. [77]
0.71	0	0.79917	0.76636
0.71	1	0.84764	0.84009
1	0	0.88783	0.87139
1	1	0.94864	0.95488
7	0	1.72583	1.72246

Table 3 Comparison of values of $\frac{Sh}{\mathrm{Re}_x^{1/2}}$ for diverse Sc, δ and γ for $\Gamma = M = K_p = R = Du = Sr = \mathrm{Pr} = 0$, $Sc = 0.6$ and $\lambda = 1$.

γ	δ	Current results	Baag et al. [77]
0	0	0.77087	0.71785
0	1	0.80470	0.76031
1	1	1.06679	1.04230
− 1	1	0.48598	0.39318

Conclusions

The current study focuses over the stagnation point flow of magnetohydrodynamic micropolar liquid to a heated area under the impacts of porous medium and thermal radiation. The study is considered under the Cartesian coordinate system. Using appropriate similarity transformations and non-dimensional quantities, the complex governing PDEs are converted to system of nonlinear coupled ODEs. Due to the complexity of the equations, we have used Mathematica software to discover the solution of the problem. The main findings of the current research are:

1. Velocity augments with the increase in concentration Grashof number, Soret number and Richardson number.
2. With the rise in chemical reaction parameter, micropolar fluid parameter and radiation parameter, the velocity of the liquid decreases.
3. Mixed behavior is observed in the microrotation with all the parameters of interest.
4. Temperature is a rising function of radiation parameter, M and γ.
5. Temperature reduces with augment of Pr, Sr and Du.
6. Concentration is a reducing function of R, M and chemical reaction parameter.

The stagnation point flow of MHD micropolar liquid past a stretching area through radiation, porous medium, heat and mass transport is very significant as many practical implications in industry. The applications include polymer sheet extrusion from a dye, metallic plate condensation process in a cooling bath and aerodynamic extrusion of sheets. The current study focused on micropolar fluid with MHD, porous medium and radiation. The future directions of the current study are: the investigators may consider micropolar nanofluid flows with electro-osmosis, activation energy, microorganisms along through slip and convective boundary conditions. These studies will lead to great importance in the industrial applications.

Acknowledgements The authors extend their appreciation to the Deanship of Scientific Research at King Khalid University, Abha, Saudi Arabia, for funding this work through the Research Group under grant number (R.G.P.2/50/ 42).

References

1. Sui J, Zhao P, Cheng Z, Doi M. Influence of particulate thermophoresis on convection heat and mass transfer in a slip flow of a viscoelasticity-based micropolar fluid. Int J Heat Mass Transfer. 2018;119:40–51.
2. Mahabaleshwar US, Sarris IE, Lorenzini G. Effect of radiation and Navier slip boundary of Walters' liquid B flow over a stretching sheet in a porous media. Int J Heat Mass Transf. 2018;127:1327–37.
3. Chiu HC, Jang JH, Yan WM. Mixed convection heat transfer in horizontal rectangular ducts with radiation effects. Int J Heat Mass Transf. 2007;50:2874–82.
4. Hayat T, Qayyum S, Alsaedi A, Shafiq A. Inclined magnetic field and heat source/sink aspects in flow of nanofluid with nonlinear thermal radiation. Int J Heat Mass Transf. 2016;103:99–107.
5. Sheikholeslami M, Ghasemi A, Li Z, Shafee A, Saleem S. Influence of CuO nanoparticles on heat transfer behavior of PCM in solidification process considering radiative source term. Int J Heat Mass Transf. 2018;126:1252–64.
6. Waqas M, Farooq M, Khan MI, Alsaedi A, Hayat T, Yasmeen T. Magnetohydrodynamic (MHD) mixed convection flow of micropolar liquid due to nonlinear stretched sheet with convective condition. Int J Heat Mass Transf. 2016;102:766–72.
7. Zheng L, Niu J, Zhang X, Mac L. Dual solutions for flow and radiative heat transfer of a micropolar fluid over stretching/shrinking sheet. Int J Heat Mass Transf. 2012;55:7577–86.
8. Hsiao KL. Micropolar nanofluid flow with MHD and viscous dissipation effects towards a stretching sheet with multimedia feature. Int J Heat Mass Transf. 2017;112:983–90.
9. Mabood F, Ibrahim SM, Rashidi MM, Shadloo MS, Lorenzini G. Non-uniform heat source/sink and Soret effects on MHD non-Darcian convective flow past a stretching sheet in a micropolar fluid with radiation. Int J Heat Mass Transf. 2016;93:674–82.
10. Bhattacharyya K, Mukhopadhyay S, Layek GC, Pop I. Effects of thermal radiation on micropolar fluid flow and heat transfer over a porous shrinking sheet. Int J Heat Mass Transf. 2012;55:2945–52.
11. Reddy MG, Sandeep N. Heat and mass transfer in radiative MHD Carreau fluid with cross diffusion. Ain Shams Eng J. 2018;9:1189–204.
12. Shateyi S, Motsa SS, Sibanda P. The effects of thermal radiation, Hall currents, Soret, and Dufour on MHD flow by mixed convection over a vertical surface in porous media. Math Problems Eng. 2010;2010:627475.
13. Pal D, Mondal H. Effects of Soret Dufour, chemical reaction and thermal radiation on MHD non-Darcy unsteady mixed convective heat and mass transfer over a stretching sheet. Commun Nonlinear Sci Numer Simul. 2011;16:1942–58.
14. Sohail M, Naz R, Abdelsalam SI. On the onset of entropy generation for a nanofluid with thermal radiation and gyrotactic microorganisms through 3D flows. Physica Scripta. 2020;95(4):045206.
15. Hayat T, Qayyum S, Waqas M, Alsaedi A. Thermally radiative stagnation point flow of Maxwell nanofluid due to unsteady convectively heated stretched surface. J Mol Liq. 2016;224:801–10.
16. Qasim M, Afridi MI, Wakif A, Saleem S. Influence of variable transport properties on nonlinear radioactive Jeffrey fluid flow over a disk: utilization of generalized differential quadrature method. Arab J Sci Eng. 2019;44(6):5987–96.
17. Dogonchi AS, Waqas M, Ganji DD. Shape effects of Copper-Oxide (CuO) nanoparticles to determine the heat transfer filled in a partially heated rhombus enclosure: CVFEM approach. Int Commun Heat Mass Transf. 2019;107:14–23.
18. Waqas M. Diffusion of stratification based chemically reactive Jeffrey liquid featuring mixed convection. Surf Interfaces. 2021;23:100783.
19. Hayat T, Khalid H, Waqas M, Alsaedi A. Numerical simulation for radiative flow of nanoliquid by rotating disk with carbon nanotubes and partial slip. Comput Methods Appl Mech Eng. 2018;341:397–408.
20. Waqas M, Hayat T, Alsaedi A. A theoretical analysis of SWCNT–MWCNT and H_2O nanofluids considering Darcy-Forchheimer relation. Appl Nanosci. 2019;9(5):1183–91.
21. Hayat T, Waqas M, Shehzad SA, Alsaedi A. Mixed convection flow of a Burgers nanofluid in the presence of stratifications and heat generation/absorption. Eur Phys J Plus. 2016;131(8):253.
22. Souayeh B, Ganesh Kumar K, Gnaneswara Reddy M, Rani S, Hdhiri N, Alfannakh H, Rahimi-Gorji M. Slip flow and radiative heat transfer behavior of Titanium alloy and ferromagnetic nanoparticles along with suspension of dusty fluid. J Mole Liq. 2019;290:111223.
23. Shafiq A, Mebarek-Oudina F, Sindhu TN, Abidi A. A study of dual stratification on stagnation point Walters' B nanofluid flow via radiative Riga plate: a statistical approach. Eur Phys J Plus. 2021;136:407. https://doi.org/10.1140/epjp/s13360-021-01394-z.

24. Hajizadeh A. Free convection flow of nanofluids between two vertical plates with damped thermal flux. J Mole Liq. 2019;289:110964.
25. Raza J, Mebarek-Oudina F, Ram P, Sharma S. MHD flow of non-Newtonian molybdenum disulfide nanofluid in a converging/diverging channel with Rosseland radiation. Defect Diffus Forum. 2020;401:92–106.
26. Kishore PM, Rajesh V, Verma SV. The effects of thermal radiation and viscous dissipation on MHD heat and mass diffusion flow past an oscillating vertical plate embedded in a porous medium with variable surface conditions. Theoret Appl Mech. 2012;39:99–125.
27. Karthikeyan S, Bhuvaneswari M, Rajan S, Sivasankaran S. Thermal radiation effects on MHD convective flowover a plate in a porous medium by perturbation technique. Appl Math Comput Intell. 2013;2(1):75–83.
28. Hossain MS, Samand MA. Heat and mass Transfer of an MHD free convection flow along a stretching sheet with chemical reaction, radiation and heat generation in presence of magnetic field. Res J Math Stat. 2013;5:5–17.
29. Hsiao KL. Nanofluid flow with multimedia physical features for conjugate mixed convection and radiation. Comput Fluids. 2014;104(20):1–8.
30. Waqas MA. Mathematical and computational framework for heat transfer analysis of ferromagnetic non-Newtonian liquid subjected to heterogeneous and homogeneous reactions. J Magn Magn Mater. 2020;493:165646.
31. Wakif A, Sehaqui R. Generalized differential quadrature scrutinization of an advanced MHD stability problem concerned water-based nanofluids with metal/metal oxide nanomaterials: a proper application of the revised two-phase nanofluid model with convective heating and through flow boundary conditions. Numer Methods Part Diff Equ. 2020. https://doi.org/10.1002/num.22671.
32. Naz R, Tariq S, Sohail M, Shah Z. Investigation of entropy generation in stratified MHD Carreau nanofluid with gyrotactic microorganisms under Von Neumann similarity transformations. Eur Phys J Plus. 2020;135(2):178.
33. Khan MI, Khan WA, Waqas M, Kadry S, Chu YM, Nazeer M. Role of dipole interactions in Darcy-Forchheimer first-order velocity slip nanofluid flow of Williamson model with Robin conditions. Appl Nanosci. 2020;10(12):5343–50.
34. Zaim A, Aissa A, Mebarek-Oudina F, Mahanthesh B, Lorenzini G, Sahnoun M. Galerkin finite element analysis of magneto-hydrodynamic natural convection of Cu-water nanoliquid in a baffled U-shaped enclosure. Propuls Power Res. 2020;9(4):383–93. https://doi.org/10.1016/j.jppr.2020.10.002.
35. Nagaraja B, Gireesha BJ. Exponential space-dependent heat generation impact on MHD convective flow of Casson fluid over a curved stretching sheet with chemical reaction. J Therm Anal Calorim. 2021;143:4071–9.
36. Bhandari A, Husain A. Optimization of heat transfer properties on ferrofluid flow over a stretching sheet in the presence of static magnetic field. J Therm Anal Calorim. 2021;144(4):1253–70.
37. Freidoonimehr N, Rahimi AB. Brownian motion effect on heat transfer of a three-dimensional nanofluid flow over a stretched sheet with velocity slip. J Therm Anal Calorim. 2019;135(1):207–22.
38. Mebarek-Oudina F, Keerthi Reddy N, Sankar M. Heat source location effects on buoyant convection of nanofluids in an annulus, advances in fluid dynamics. Lecture Notes Mech Eng. 2021. https://doi.org/10.1007/978-981-15-4308-1_70.
39. Sohail M, Naz R, Shah Z, Kumam P, Thounthong P. Exploration of temperature dependent thermophysical characteristics of yield exhibiting non-Newtonian fluid flow under gyrotactic microorganisms. AIP Adv. 2019;9(12):125016.
40. Zaim A, Aissa A, Mebarek-Oudina F, Rashad MA, Hafiz MA, Sahnoun M, El Ganaoui M. Magnetohydrodynamic natural convection of hybrid nanofluid in a porous enclosure: numerical analysis of the entropy generation. J Therm Anal Calorim. 2020;141(5):1981–92. https://doi.org/10.1007/s10973-020-09690-z.
41. Mebarek-Oudina F, Fares R, Aissa A, Lewis RW, H. Abu-Hamdeh N. Entropy and convection effect on magnetized hybrid nano-liquid flow inside a trapezoidal cavity with zigzagged wall. Int Commun Heat Mass Trans. 2021;125:105279. https://doi.org/10.1016/j.icheatmasstransfer.2021.105279.
42. Alkasassbeh M, Omar Z, Mebarek-Oudina F, Raza J, Chamkha AJ. Heat transfer study of convective fin with temperature-dependent internal heat generation by hybrid block method. Heat Transfer-Asian Res. 2019;48(4):1224–47. https://doi.org/10.1002/htj.21428.
43. Khan U, Zaib A, Mebarek-Oudina F. Mixed convective magneto flow of SiO2–$MoS_2/C_2H_6O_2$ hybrid nanoliquids through a vertical stretching/shrinking wedge: stability analysis. Arab J Sci Eng. 2020;45:9061–73. https://doi.org/10.1007/s13369-020-04680-7.
44. Kahshan M, Lu D, Rahimi-Gorji M. Hydrodynamical study of flow in a permeable channel: application to flat plate dialyzer. Int J Hydrogen Energy. 2019;44(31):17041–7.
45. Marzougui S, Mebarek-Oudina F, Aissa A, Magherbi M, Shah Z, Ramesh K. Entropy generation on magneto-convective flow of copper-water nanofluid in a cavity with chamfers. J Therm Anal Calorim. 2021;143(3):2203–14. https://doi.org/10.1007/s10973-020-09662-3.
46. Ganesh Kumar K, Avinash BS, Rahimi-Gorji M, Alarifi IM. Optical and electrical properties of $Ti_{1-X}Sn_XO_2$ nanoparticles. J Mole Liq. 2019;293:111556.
47. Sohail M, Naz R, Abdelsalam SI. Application of non-Fourier double diffusions theories to the boundary-layer flow of a yield stress exhibiting fluid model. Physica A Stat Mech Appl. 2020;537:122753.
48. Sohail M, Naz R. Modified heat and mass transmission models in the magnetohydrodynamic flow of Sutterbynanofluid in stretching cylinder. Physica A Stat Mech Appl. 2020;549:124088.
49. Fares R, Mebarek-Oudina F, Aissa A, Bilal SM, Öztop HF. Optimal entropy generation in darcy-forchheimer magnetized flow in a square enclosure filled with silver based water nanoliquid. J Therm Anal Calorim. 2021. https://doi.org/10.1007/s10973-020-10518-z.
50. Bilal S, Sohail M, Naz R. Heat transport in the convective Casson fluid flow with homogeneous-heterogeneous reactions in Darcy-Forchheimer medium. Multidiscip Model Mater Struct. 2019;15(6):1170–89.
51. Bilal S, Sohail M, Naz R, Malik MY, Alghamdi M. Upshot of ohmically dissipated Darcy-Forchheimer slip flow of magnetohydrodynamic Sutter by fluid over radiating linearly stretched surface in view of Cash and Carp method. Appl Math Mech. 2019;40(6):861–76.
52. Ashraf MU, Qasim M, Wakif A, Afridi MI, Animasaun IL. A generalized differential quadrature algorithm for simulating magnetohydrodynamic peristaltic flow of blood-based nanofluid containing magnetite nanoparticles: a physiological application. Numer Methods Part Diff Equ. 2020. https://doi.org/10.1002/num.22676.
53. Wakif A, Chamkha A, Animasaun IL, Zaydan M, Waqas H, Sehaqui R. Novel physical insights into the thermodynamic irreversibilities within dissipative EMHD fluid flows past over a moving horizontal riga plate in the coexistence of wall suction and joule heating effects: a comprehensive numerical investigation. Arab J Sci Eng. 2020;45(11):9423–38.
54. Qasim M, Ali Z, Wakif A, Boulahia Z. Numerical simulation of MHD peristaltic flow with variable electrical conductivity and Joule dissipation using generalized differential quadrature method. Commun Theor Phys. 2019;71(5):509.

55. Wakif A, Qasim M, Afridi MI, Saleem S, Al-Qarni MM. Numerical examination of the entropic energy harvesting in a magnetohydrodynamic dissipative flow of Stokes' second problem: utilization of the gear-generalized differential quadrature method. J Non-Equilib Thermodyn. 2019;44(4):385–403.
56. Dadheech PK, Agrawal P, Mebarek-Oudina F, Abu-Hamdeh N, Sharma A. Comparative heat transfer analysis of $MoS_2/C_2H_6O_2$ and MoS_2- SiO_2/ $C_2H_6O_2$ nanofluids with natural convection and inclined magnetic field. J Nanofluids. 2020; 9(3):161–167. https://doi.org/10.1166/jon.2020.1741
57. Marzougui S, Bouabid M, Mebarek-Oudina F, Abu-Hamdeh N, Magherbi M, Ramesh K. A computational analysis of heat transport irreversibility phenomenon in a magnetized porous channel. Int J Numer Meth Heat Fluid Flow. 2020. https://doi.org/10.1108/HFF-07-2020-0418.
58. Seikh AH, Adeyeye O, Omar Z, Raza J, Rahimi-Gorji M, Alharthi N, Khan I. Enactment of implicit two-step Obrechkoff-type block method on unsteady sedimentation analysis of spherical particles in Newtonian fluid media. J Mole Liq. 2019;293:111416.
59. Swain K, Mebarek-Oudina F, Abo-Dahab SM. Influence of MWCNT/Fe_3O_4 hybrid-nanoparticles on an exponentially porous shrinking sheet with variable magnetic field and chemical reaction. J Therm Anal Calorim. 2021. https://doi.org/10.1007/s10973-020-10432-4.
60. Mebarek-Oudina F. Numerical modeling of the hydrodynamic stability in vertical annulus with heat source of different lengths. Eng Sci Technol. 2017;20(4):1324–33.
61. Abo-Dahab SM, Abdelhafez MA, Mebarek-Oudina F, Bilal SM. MHD Casson nanofluid flow over nonlinearly heated porous medium in presence of extending surface effect with suction/injection. Indian J Phys. 2021. https://doi.org/10.1007/s12648-020-01923-z.
62. Mebarek-Oudina F. Convective heat transfer of titania nanofluids of different base fluids in cylindrical annulus with discrete heat Source. Heat Transfer-Asian Res. 2019;48:135–47.
63. Mebarek-Oudina F, Bessaih R, Mahanthesh B, Chamkha AJ, Raza J. Magneto-thermal-convection stability in an inclined cylindrical annulus filled with a molten metal. Int J Numer Meth Heat Fluid Flow. 2020;31(4):1172–89.
64. Kumar KA, Sugunamma V, Sandeep N. Effect of thermal radiation on MHD Casson fluid flow over an exponentially stretching curved sheet. J Therm Anal Calorim. 2020;140(5):2377–85.
65. Golafshan B, Rahimi AB. Effects of radiation on mixed convection stagnation-point flow of MHD third-grade nanofluid over a vertical stretching sheet. J Therm Anal Calorim. 2019;135(1):533–49.
66. Dutta A, Chattopadhyay H, Yasmin H, Rahimi-Gorji M. Entropy generation in the human lung due to effect of psychrometric condition and friction in the respiratory tract. Comput Methods Programs Biomed. 2019;180:105010.
67. Waqas M, Jabeen S, Hayat T, Khan MI, Alsaedi A. Modeling and analysis for magnetic dipole impact in nonlinear thermally radiating Carreau nanofluid flow subject to heat generation. J Magn Magn Mater. 2019;485:197–204.
68. Rajashekhar C, Mebarek-Oudina F, Vaidya H, Prasad KV, Manjunatha G, Balachandra H. Mass and heat transport impact on the peristaltic flow of Ree-Eyring liquid with variable properties for hemodynamic flow. Heat Transf. 2021. https://doi.org/10.1002/htj.22117.
69. Thumma T, Wakif A, Animasaun IL. Generalized differential quadrature analysis of unsteady three-dimensional MHD radiating dissipative Casson fluid conveying tiny particles. Heat Transf. 2020;49(5):2595–626.
70. Raza J, Mebarek-Oudina F, Chamkha AJ. Magnetohydrodynamic flow of molybdenum disulfide nanofluid in a channel with shape effects. Multidiscip Model Mater Struct. 2019;15(4):737–57.
71. Swain K, Mahanthesh B, Mebarek-Oudina F. Heat transport and stagnation-point flow of magnetized nanoliquid with variable thermal conductivity with Brownian moment and thermophoresis aspects. Heat Transf. 2021;50:754–67.
72. Wakif A, Chamkha A, Thumma T, Animasaun IL, Sehaqui R. Thermal radiation and surface roughness effects on the thermo-magneto-hydrodynamic stability of alumina–copper oxide hybrid nanofluids utilizing the generalized Buongiorno's nanofluid model. J Therm Anal Calorim. 2021;143:1201–20.
73. Mebarek-Oudina F, Aissa A, Mahanthesh B, Oztop HF. Heat transport of magnetized newtonian nanoliquids in an annular space between porous vertical cylinders with discrete heat source. Int Comm Heat Mass Transf. 2020;117:104737. https://doi.org/10.1016/j.icheatmasstransfer.2020.104737.
74. Djebali R, Mebarek-Oudina F, Choudhari R. Similaritysolution analysis of dynamic and thermal boundary layers: further formulation along a vertical flat plate. Physica Scripta. 2021;96(8):085206. https://doi.org/10.1088/1402-4896/abfe31.
75. Aman F, Ishak A, Pop I. MHD stagnation point flow of a micropolar fluid toward a vertical plate with a convective surface boundary condition. Bull Malaysian Math Sci Soc. 2013;36(4):865–79.
76. Makinde OD, Khan WA, Khan ZH. Stagnation point flow of MHD chemically reacting nanofluid over a stretching convective surface with slip and radiative heat. Proc Inst Mech Eng Part E J Process Mech Eng. 2017;231(4):695–703.
77. Baag S, Mishra SR, Dash GC, Acharya MR. Numerical investigation on MHD micropolar fluid flow toward a stagnation point on a vertical surface with heat source and chemical reaction. J King Saud Univ-Eng Sci. 2017;29(1):75–83.